THE JOURNAL OF PHYSICAL CHEMISTRY C LETTERS

2007, *111,* 17985−17988
Published on Web 11/08/2007

Surface-Enhanced Raman Spectroscopy and Nanogeometry: The Plasmonic Origin of SERS

Seung Joon Lee,[†] Zhiqiang Guan,[‡] Hongxing Xu,[‡] and Martin Moskovits*[,†]

Department of Chemistry & Biochemistry, University of California, Santa Barbara, California 93106, and Institute of Physics, Chinese Academy of Sciences, Box 603-146, Beijing 100080, China

Received: September 14, 2007; In Final Form: October 18, 2007

Using a series of highly regular nanostructures consisting of periodic Ag nanowires fabricated in porous aluminum oxide, we validate the overwhelmingly plasmonic origin of the most intense SERS signals such as those responsible for single-molecule SERS, demonstrating its sensitive dependence on the system's nanogeometry. By varying the interwire gap distance from 35 to 10 nm, the SERS intensity excited with 785 nm laser light, increased over 200-fold. These observations were shown to agree quantitatively with electromagnetic field calculations carried out using the free space green's tensor method.

Introduction

Although surface-enhanced Raman spectroscopy (SERS) was discovered some 30 years ago[1] and its plasmonic origin of the enhancement substantially formulated at approximately the same time, the primary cause of the largest reported signal enhancements ($\sim 10^{14}$),[2,3] high enough for single-molecule detection, has been the subject of continuous discussion. These large enhancements are normally attributed to highly concentrated electromagnetic (EM) fields associated with strong localized surface plasmon resonances at interstitial sites (so-called EM or SERS hot spots) in nanostructures consisting of two or more coupled nanoparticles or nanostructured surfaces with closely spaced features.[4,5] Many theoretical and computational studies[5,6] have shown how the aforementioned field concentration depends on such parameters as the specific geometry of the nanostructured site where the probed molecules reside, the wavelength, and the polarization of the incident laser light. However, few experimental studies have appeared that demonstrate a substantial increase in the SERS intensity as a function of *physical* parameters such as the nanogeometry of the structures involved. This is what we show herein, using a series of high-order, periodic silver nanostructures in which effectively only geometrical parameters vary. By changing the internanowire gap distance from 35 to 10 nm, SERS intensity excited with 785 nm, increased over 200-fold. The experimental results were shown to agree quantitatively with calculation using the free space green's tensor method. This observation demonstrates the overwhelmingly plasmonic origin of SERS and validates an entire generation of calculations that have hitherto received only cursory systematic experimental testing. They also demonstrate just how sensitively the EM enhancement depends on the nanogeometrical details of the system (not unexpectedly because surface-plasmon resonances arise from continuity relations across interfaces).

Experimental Methods

Sample Preparation. High-order porous anodic oxide (PAO) templates were prepared by anodizing ultrahigh-purity aluminum in oxalic acid. The anodizing was carried out at 40 V dc at 15−17 °C. A 1-h second anodizing resulted in a template with nanochannel depth of ~ 5 μm. A third anodization was carried out in 0.2 M phosphoric acid for 10 min under the same conditions in order to reduce the barrier layer thickness, facilitating Ag deposition. The PAO pores were widened in 0.5 M phosphoric acid at 40 °C for a variable time to achieve varying pore diameters. For a given pore density, corresponding in our samples to a 100 nm center-to-center distance between pores (d_{cc}, Figure 1 in the main article), the pore diameter (D_{diam}) increases as the pore-widening proceeds; at the same time, the neighboring pore-wall thickness decreases. These will translate into variable nanowire diameters (D_{diam}) and interwire gap distances ($d_{gap} = d_{cc} - D_{diam}$ in Figure 1). Samples with d_{gap} values of 35 ± 5, 30 ± 5, 23 ± 6, 19 ± 3, 14 ± 3, 10 ± 2, and 8 ± 2 nm were produced. Templates with d_{gap} below 10 nm were hard to produce reproducibly partly because of the collapse of the PAO channels caused by uneven etching along the wall at such small values of the wall thickness. Accordingly, $d_{gap} \sim 10$ nm is the smallest practical gap size attainable by our fabrication method. Ag deposition was carried out at room temperature using AC electrolysis in an electrolyte composed of 0.05 M $AgNO_3$ + 0.5 M H_3BO_3.

Raman Spectroscopy. 4-aminobenzenethiol (4-ABT) was dosed onto the exposed tips of the Ag nanowire as a Raman probe, and SERS measurements were carried out at 514.5 and 785 nm. All of the samples showed strong SERS emissions. Backscattered Raman spectra were recorded on a LabRam microRaman system (Jobin-Yvon/ISA) equipped with a thermoelectrically cooled CCD detector. Continuous wave 514.5 nm (SpectraPhysics 164) and 785 nm wavelengths were used

* To whom correspondence should be addressed. E-mail: mmoskovits@ltsc.ucsb.edu.
[†] University of California.
[‡] Chinese Academy of Sciences.

10.1021/jp077422g CCC: $37.00

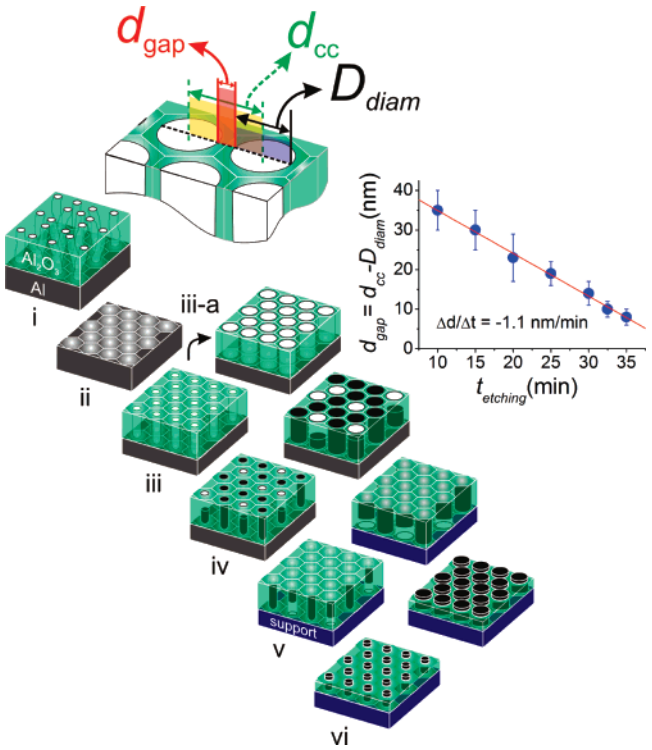

Figure 1. Schematic illustrating the fabrication of SERS systems consisting of periodically disposed Ag nanowires embedded in highly regular porous aluminum oxide (PAO) templates with varying interwire gap distances, d_{gap}. PAO were electrochemically fabricated on an aluminum sheet in 0.3 M oxalic acid using Masuda's two-step anodizing process (i through iii).[8] This was followed by pore-widening in 0.5 M phosphoric acid (iii to iii-a). Pore-widening was carried out so as to create templates with d_{gap} values of 35 ± 5, 30 ± 5, 23 ± 6, 19 ± 3, 14 ± 3, 10 ± 2, and 8 ± 2 nm. The etching rate ($\Delta d_{gap}/\Delta t_{etch}$) was experimentally found to be ~1.1 nm/min (inset). Ag deposition was carried out at room temperature by AC electrolysis (iv). The Ag-PAO samples were epoxy glued to a Si wafer (oxide-side down) and the aluminum on the backside of Ag-PAO was removed by etching in saturated $HgCl_2$ for 1 h (iv to v). The alumina matrix surrounding the silver nanowires was partially etched in 0.1 M aqueous NaOH for ~10−12 min to expose approximately 50 nm of the tips of AgNWs (vi).[14]

to excite samples. The red excitation was provided by a Ti:Sapph laser (SpectraPhysics 3900s) set at 785 nm and pumped by a 2 W of Ar ion laser operating in a multiline mode.

Electromagnetic Field Calculations. The local EM fields were calculated using the free-space green's tensor method,[7] which allows the local EM fields to be computed in the vicinity of nanostructures with arbitrary shapes, sizes, and configurations. The array of AgNWs was approximated by a central nanodisc surrounded by six hexagonally arranged discs using dimensional parameters (disc-to-disc distance and disc diameter) equal to the mean values of the AgNWs produced experimentally. The disc height was taken to be 50 nm, and the light (alternately at 785 and 514.5 nm) was assumed to be directed such that its wave vector was parallel to the nanodisc's cylindrical axis. Aside from the obvious approximation that a large two-dimensional (2D) array was mimicked by a seven-element cluster, the approximation that the tips of the AgNWs that had been etched out of the aluminum oxide matrix could be approximated using discs is a significant approximation because we showed that the field strengths depend significantly on the cylinder heights as well as on the fact that there is an oxide matrix surrounding the lower portion of the AgNWs. Nevertheless, the results are gratifying. The EM enhancement factors are calculated using eq 1

$$G_{SERS} = |E(\lambda)/E_0(\lambda)|^2 |E(\lambda')/E_0(\lambda')|^2 \quad (1)$$

where λ and λ' are the incident and Stokes-shifted wavelengths, respectively. The average EM enhancement factor at various points on the surface of the central cylinder was averaged using the function (eq 2)

$$\bar{G} = \langle G_{loc} \rangle = \frac{\sum_{n_{-grid}} G_{loc}}{n_{-grid}} \quad (2)$$

where for simplicity the local enhancement was assumed to be related to the local electric field as eq 3

$$G_{loc} = |E_{loc}(\lambda)/E_0(\lambda)|^4 \quad (3)$$

We assumed that the molecules are adsorbed on the tops and side walls of the cylinders and therefore carried out the field averages over these surfaces. By following this prescription, all of the essential geometrical parameters: the nanowire diameter, height, and interwire gap distances were taken into account for each of the samples. Likewise, the different surface areas of the samples used and therefore the differing numbers of molecules adsorbed on each sample were also automatically included in the calculation. The experimental data was compared with the calculated results by scaling the latter so as to bring the two sets of values into approximate coincidence for the midrange gap values. The robustness of the calculations was tested by comparing the E-field results obtained on arrays of silver spheres using the free-space green's tensor method with those calculated by the generalized Mie theory. The two methods produced very similar results.[8]

Results and Discussion

One of the facts that is often insufficiently emphasized is that most SERS observations cannot be understood in terms of simple, isolated nanoparticles. It is the complex, near-field interactions among nanostructures that produce so-called EM hot spots,[4,5] from where the largest SERS enhancements originate because of a very great concentration both of the incident and Raman-scattered optical fields. This picture arises primarily from theory, which, for example, predicts an increase of several orders of magnitude in SERS enhancement when, for example, the gap distance between two nanoparticles is reduced by an order of magnitude. Experimental verifications of these predictions have normally reported intensity changes of the order of 10−20. This limited range has been credibly ascribed to experimental realities: the difficulty of creating nanostructures with small, controllable nanogap distances, the problem of squeezing a scanning nanoprobe into an EM hot spot, and so on. All the same, experimental verification of the predicted dramatic effects of nanogeometry on SERS remains very sparse.

Periodic 2D arrays of silver nanowires (AgNWs) with good wire-to-wire diameter reproducibility and periodic domains extending over areas tens of square micrometers were electrochemically produced in porous aluminum oxide (PAO) templates. The internanowire gaps are theoretically predicted to be SERS hot spots whose enhancing abilities can be varied systematically and dramatically using template-assisted control of the interwire spacing. The series of hexagonally periodic Ag

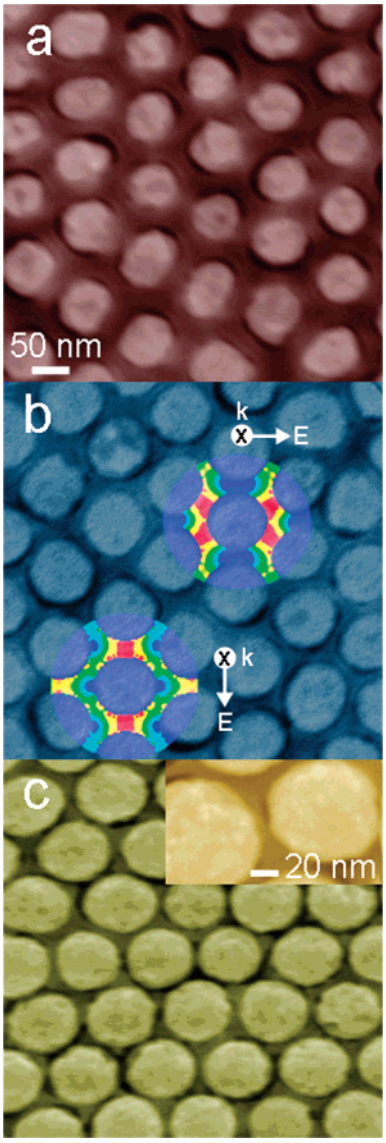

Figure 2. SEM images (FEI XL 40) of Ag-PAO templates with d_{gap} of (a) 35 ± 5, (b) 19 ± 3, and (c) 10 ± 2 nm. (The 50 nm scale bar applies to all three images.) The calculated local EM field amplitudes in the vicinity of a central nanodisc surrounded by six hexagonally arranged discs are superimposed on the SEM figures in b. The parameters d_{gap} = 20 nm, D_{diam} = 80 nm, and λ_{ex} = 785 nm were assumed in the calculation; *k* and *E* indicate, respectively, the wavevector and electric vector directions of the incident light. The inset in c shows a magnification of a portion of the image shown in c.

nanostructures fabricated with interwire gap distances (d_{gap}) varying from 35 to 10 nm showed intense SERS activity with enhancements varying by a factor of over 200.

Figure 1 illustrates the experimental strategy schematically.[9,10] Prior to AgNW deposition, the PAO templates were etched in 0.5 M phosphoric acid at 40 °C for a variable time resulting in pores of progressively larger (but uniform) diameter and a decreasing pore-wall thickness between pores. SEM images of three of the experimental samples with interwire gap distances of (a) 35 nm, (b) 19 nm, and (c) 10 nm are shown in Figure 2. The high-order, hexagonal periodicity is clearly visible. The simultaneous variation of the nanowire diameter, D_{diam}, and d_{gap} is not a problem because both parameters are purely geometrical factors and both are appropriately considered in the calculations.

Figure 3a and b shows the SERS spectra of 4-ABT recorded as a function of d_{gap}. At 785 nm excitation, the SERS intensity increases dramatically as the d_{gap} decreases. The dependence

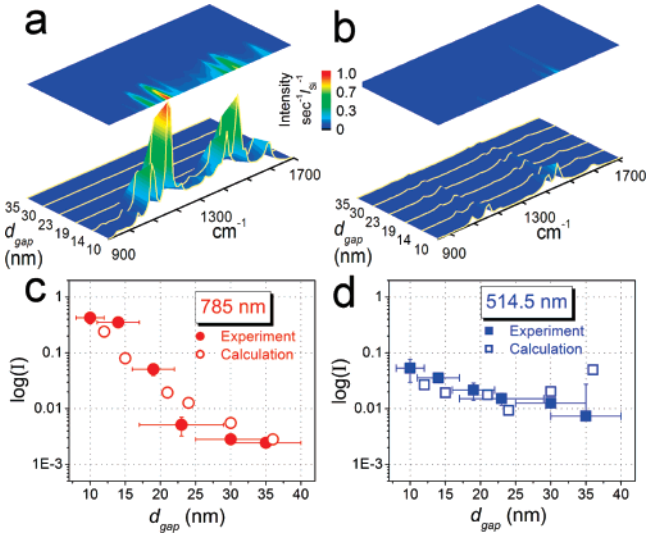

Figure 3. SERS spectra and corresponding 2D intensity contour maps of 4-aminobenzenethiol (4-ABT) adsorbed on the Ag-PAO nanoarrays are shown as a function of d_{gap}. Spectrum and 2D contour map excited with (a) 785 nm and (b) 514.5 nm. The prominent bands observed at 1580, 1438, 1390, 1142, and 1078 cm^{-1} are due to benzene ring vibrations.[15] The Si band at 520 cm^{-1} was used as a calibration marker to correct for the spectrometer's response at the two wavelengths. Experimentally measured (filled points) and calculated (open points) intensities of the 1078 cm^{-1} SERS line of 4-ABT plotted as a function of the interwire gap size are shown in c and d, respectively, for 785 and 514.5 nm excitation. Logarithms of the intensities are plotted so as to compress the intensity scale. The error bars for the log(*I*) scale are shown for those points for which the error exceeds the size of the point.

on gap size is less pronounced when the nanostructure is excited with 514.5 nm. For example, with 514.5 nm excitation the SERS intensity at 1078 cm^{-1} decreases by a factor of ~7 on going from d_{gap} = 10 nm to d_{gap} = 35 nm. In contrast, at 785 nm excitation the SERS intensity decreased by a factor of ~200 on going from the former to the latter sample. These observations agree well with the calculated values at both excitation wavelengths (Figure 3c and d). This agreement is better for red (λ_{ex} = 785 nm) excitation than for green (λ_{ex} = 514.5 nm). This is expected. The wavelength dependence of the field strength is far more complex in the green portion of the spectrum[11] and therefore much more sensitive to small variations between the true geometry of the NWs and the ideally circular geometry assumed in the calculations.

Overlaid on the SEM image in Figure 2b are contour maps of the calculated local EM field amplitudes in the vicinity of a group of seven 80 nm diameter (i.e., d_{gap} = 20 nm) cylinders simulated at two orthogonal polarizations and λ_{ex} = 785 nm. Although the location of the hot spots changes with the polarization of the incident light used, the EM enhancements averaged over all of the surfaces of the nanostructures is approximately constant, independent of the polarization. (The calculated field distributions at the two wavelengths and for two polarizations are given in the Supporting Information.) This situation differs from what is expected for one or a few molecules localized, for example, in the interstice between two nanoparticles where polarization is expected to be a significant factor determining SERS enhancement.[3,12]

These results confirm the fundamentally plasmonic origin of even the most intense SERS signals,[1] the salient features of which are already there for a two-nanoparticle system (or for a core−shell particle). The key elements of this phenomenon persist for larger clusters as is shown in Figure 2b. This accounts

fully for the observation that for the 2D arrays with the largest internanowire gap ($d_{gap} = 35$ nm) the SERS intensity at 1078 cm^{-1} is ~3 times stronger with 514.5 nm excitation than that using 785 nm, whereas at the smallest gap ($d_{gap} = 10$ nm) the SERS signal intensity is ~10 times stronger for red excitation as compared to green (Figure 3). This is also consistent with the observation that in isolated pairs of Ag nanodisks with diameters of ~95 nm and gaps of ~10 nm, fabricated by electron beam lithography the plasmon resonance band along the interparticle axis was found to lie in the 700 and 800 nm range.[13] In the 2D periodic metal nanoparticle arrays, the resonance conditions are particularly sensitive to the geometrical parameters (D_{diam} and d_{gap}) and long-range order for high EM enhancement.[11] When the diameter (D_{diam}) is larger than the gap size (d_{gap}) so that the when the parameter $D_{diam}/d_{gap} \gg 1$, local EM fields of high intensity are produced over a wide range of excitation wavelengths. This observation acts as a simple guide in designing optimal SERS systems based on coupled nanoparticles. Those with D_{diam}/d_{gap} values ranging from ~2 to ~9 are expected to yield strong SERS signals (when excited with an appropriate wavelength).

Conclusions

We demonstrate the overwhelmingly plasmonic origin of the most intense SERS signals and show the sensitive dependence of SERS on the system's nanogeometry. We do this by fabricating a series of periodic SERS-active Ag nanowires embedded in highly ordered porous aluminum oxide in which the interwire gap distance was varied from 35 to 10 nm. The SERS response of a probe molecule introduced into the gaps of these systems was measured at 514.5 and 785 nm. At the latter, the SERS intensity varied by a factor of more than 200 on going from 35 to 10 nm. These observations agree quantitatively with calculations using the free space green's tensor method.

Acknowledgment. Funding from the Institute for Collaborative Biotechnologies (ICB) through grant DAAD19-03-D-0004 from U.S. Army Research Office, from Lawrence Livermore National Laboratories through a UCDRD grant, and from the NSF (DMR-0097611) is gratefully acknowledged.

Supporting Information Available: Additional figure of the distributions of the EM field values calculated for 514.5 and 785 nm and assuming two orthogonal incident light polarization on the seven-disc array used to mimic the experimentally produced results. This material is available free of charge via the Internet at http://pubs.acs.org.

References and Notes

(1) (a) Fleischman, M. P.; Hendra, J.; McQuillan, A. *Chem. Phys. Lett.* **1974**, *26*, 163−166. (b) Jeanmaire, D. L.; Van, Duyne, R. P. *J. Electroanal. Chem.* **1977**, *84*, 1−20. (c) Albrecht, M. G.; Creighton, J. A. *J. Am. Chem. Soc.* **1977**, *99*, 5215−5217.

(2) Nie, S.; Emory, S. R. *Science* **1997**, *275*, 1102−1106.

(3) Kneipp, K.; Wang, Y.; Kneipp, H.; Itzkan, I.; Dasari, R. R.; Feld, M. S. *Phys. Rev. Lett.* **1996**, *76*, 2444−2447.

(4) Moskovits, M. *Rev. Mod. Phys.* **1985**, *57*, 783−826.

(5) Prodan, E. M.; Radloff, C.; Halas, N. J.; Nordlander, P. *Science* **2003**, *302*, 419−422.

(6) (a) Garcia-Vidal, F. J.; Pendry, J. B. *Phys. Rev. Lett.* **1996**, *77*, 1163−1166. (b) Xu, H.; Käll, M. *ChemPhysChem* **2003**, *4*, 1001−1005. (c) Xu, H.; Aizpurua, J.; Käll, M.; Apell, P. *Phys. Rev. E* **2000**, *62*, 4318−4324. (d) Aravind, P. K.; Nitzan, A.; Metiu, H. *Surf. Sci.* **1981**, *110*, 189−204. (e) Aravind, P. K.; Metiu, H. *J. Phys. Chem.* **1982**, *86*, 5076−5084. (f) Aravind, P. K.; Metiu, H. *Surf. Sci.* **1983**, *124*, 506−528.

(7) Martin, O. J. F.; Girard, C.; Dereux, A. *Phys. Rev. Lett.* **1995**, *74*, 526−529.

(8) Xu, H. *J. Opt. Soc. Am. A* **2004**, *21*, 804−809.

(9) Masuda, H.; Fukuda, K. *Science* **1995**, *268*, 1466−1468.

(10) Al-Mawlawi, D.; Liu, C. Z.; Moskovits, M. *J. Mater. Res.* **1994**, *9*, 1014−1018.

(11) Genov, D. A.; Sarychev, A. K.; Shalaev, V. M.; Wei, A. *Nano Lett.* **2004**, *4*, 153−158.

(12) (a) Kneipp, K.; Kneipp, H.; Kartha, V. B.; Manoharan, R.; Deinum, G.; Itzkan, I.; Dasari, R. R.; Feld, M. S. *Phys. Rev. E* **1998**, *57*, R6281−R6284. (b) Kneipp, K.; Wang, Y.; Kneipp, H.; Perelman, L. T.; Itzkan, I.; Dasari, R. R.; Feld, M. S. *Phys. Rev. Lett.* **1997**, *78*, 1667−1670. (c) Xu, H.; Bjerneld, E. J.; Käll, M.; Borjesson, L. *Phys. Rev. Lett.* **1999**, *83*, 4357−4360. (d) Gunnarsson, L.; Petronis, S.; Kasemo, B.; Xu, H.; Bjerneld, J.; Käll, M. *Nanostruct. Mater.* **1999**, *12*, 783−788. (e) Bosnick, K. A.; Jiang, J.; Brus, L. *J. Phys. Chem. B* **2002**, *106*, 8096−8099. (f) Michaels, A. M.; Jiang, J.; Brus, L. *J. Phys. Chem. B* **2000**, *104*, 11965−11971.

(13) Gunnarsson, L.; Rindzevicius, T.; Prikulis, J.; Kasemo, K.; Käll, M.; Zou, S.; Schatz, G. C. *J. Phys. Chem. B* **2005**, *109*, 1079−1087.

(14) Lee, S. J.; Morill, A. R.; Moskovits, M. *J. Am. Chem. Soc.* **2006**, *128*, 2200−2201.

(15) (a) Osawa, M.; Matsuda, N.; Yoshii, K.; Uchida, I. *J. Phys. Chem.* **1994**, *98*, 12702−12707. (b) Kim, K.; Yoon, J. K. *J. Phys. Chem. B* **2005**, *109*, 20731−20736.